EurJIC
European Journal of Inorganic Chemistry

Minireviews
doi.org/10.1002/ejic.202100635

Chemistry Europe
European Chemical Societies Publishing

VIP *Very Important Paper*

New Paradigms in Porous Framework Materials for Acetylene Storage and Separation

Gaurav Verma,[a] Junyu Ren,[a] Sanjay Kumar,[b] and Shengqian Ma*[a]

Acetylene is an important precursor in the petrochemical, plastics and electronic industries, as well as the prominent fuel for welding and metal cutting. The high flammability and explosive nature of acetylene, however hinder its safe storage and transportation. Porous materials are highly promising for acetylene storage and as they can provide strong binding interactions and an optimal pore environment. Furthermore, high selectivity and separation can be achieved for acetylene over other gases such as CO_2 and small hydrocarbons. In this review, we divulge into the recent advancements and paradigms in acetylene storage and separation with a focus on porous metal-organic frameworks (MOFs). An overview of the benchmark materials for acetylene storage and separation, along with some recent developments in the strategies to balance the trade-off between the uptake capacity and selectivity is provided. The approaches of designing small pores and highly functionalized pore environments for strong binding with the acetylene adsorbate; along with the pore space partition, window space directed assembly and inverse CO_2/C_2H_2 adsorption for the separation of acetylene from CO_2, CH_4, C_2H_4 and other hydrocarbons are reviewed to provide a summary and help further augment the research in this direction.

1. Introduction

From its early use as an illuminant for trains and city streets, acetylene is now one of the most vital components of the modern industry, serving as a raw material for the production of fine chemicals, electric materials, in welding processes and more recently in fuel cell vehicles.[1] However, its high flammability, instability, explosive nature and incompressibility pose substantial challenges regarding the safe storage and transportation of acetylene. Its storage at pressures above 2 bar is an explosion risk, even in the absence of oxygen and the current method involves dissolution of acetylene in acetone and transferring to specialized containers along with an adsorbent.[1a] However, this technique suffers from the disadvantages of low acetylene purity, high input cost and a low efficiency.

Further, the general methods of acetylene preparation (reacting calcium carbide with water, partial combustion of methane, ethylene steam cracking) usually result in the formation of several other gaseous impurities, such as methane, carbon dioxide, ethylene and other small hydrocarbons.[1b] Also, acetylene is present as a trace impurity in several petrochemicals and should be reduced to a permissible level. The similar molecular dimensions and physical properties (Table 1) render the separation of these gases quite challenging. Thus, it becomes imperative to explore and discover new materials for safe storage, delivery and effective separation of acetylene.

Table 1. A comparison of the physical properties of acetylene, methane, carbon dioxide and ethylene.[9k,m]

Gas	Dimensions [Å]	Melting point [°C]	Boiling Point [°C]	Polarizability [$\times 10^{25}$ cm^3]
C_2H_2	3.32×3.34×5.70	−84	−84	33.3–39.3
CO_2	3.18×3.33×5.36	−78.5	−78.5	25.07
CH_4	3.82×3.94×4.10	−182.5	−161.6	25.93
C_2H_4	3.28×4.18×4.84	−169.2	−103.8	42.52

Porous materials are particularly promising in this regard, owing to their high surface areas, accessible pores and their applications in gas storage. Since the first report of acetylene storage in a metal-organic framework (MOF) by Kitagawa and coworkers in 2005;[2] numerous MOFs, metal-organic containers (MOCs)[3] porous organic materials[4] such as porous organic cages (POCs)[5] and covalent organic frameworks (COFs)[6] have been reported for its storage and separation applications. MOFs, built from the assembly of metal cluster based secondary building units (SBUs) and organic linkers,[7] have distinctively heralded the research in this direction owing to their extremely high surface areas, tunable pore dimensions, ease of functionalization and a high density of active sites for strong binding interactions.[8] The past decade has seen an explosive growth in acetylene storage and separation applications, with reports of various benchmark materials exhibiting high uptake capacities and exceptional selectivities; and several critical reviews highlighting the advancements in this field.[9]

In this review, we have summarized the recent progress and new developments in achieving highly efficient acetylene storage and separation. Due to the scope of the review, we have focused our attention to MOFs. We first begin by discussing the benchmark materials in acetylene storage and

[a] *Dr. G. Verma, J. Ren, Prof. S. Ma*
Department of Chemistry,
University of North Texas
1508 W Mulberry St, Denton, TX 76201, USA
E-mail: Shengqian.Ma@unt.edu
http://www.chemistry.unt.edu/~sqma/
[b] *Dr. S. Kumar*
Department of Chemistry,
Multani Mal Modi College
Patiala 147001, Punjab, India

some of the latest strategies to enhance the uptake capacities, followed by a focus on the milestones achieved in separation of acetylene from CO_2, CH_4, C_2H_4 and other hydrocarbons; and we conclude by discussing the challenges in practical applications and future directions.

2. Acetylene Storage in MOFs

Kitagawa and coworkers were the first to explore MOFs for acetylene storage.[2] In 2005, they reported $[Cu_2(pzdc)_2(pyz)]$ (pzdc: pyrazine-2,3-dicarboxylate, pyz: pyrazine) featuring suitable pore channels (4 Å × 6 Å) and oxygen functionalities (as basic adsorption sites) decorating the pore surface. The material exhibited a saturated adsorption capacity of 42 cm^3 (STP) g^{-1} and a high affinity for acetylene with a Q_{st} value of 42.5 kJ mol^{-1}. A dense packing of the acetylene molecules in the channels was observed with the hydrogens of the C_2H_2 interacting with the uncoordinated carbonyl oxygen atoms on the pore wall, resulting in a confinement effect. This work drew the attention of researchers towards applicability of MOFs in acetylene storage and the field has since greatly expanded, with significant advancements made regarding enhancing the uptake and tuning the adsorption properties by an understanding of the interactions involved.

In 2009, Xiang et al. examined six MOFs: MOF-505, MOF-508, MOF-5, MIL-53, ZIF-8 and HKUST-1 having varied structures and porosities for their acetylene adsorption performance (Figure 1). The materials could be categorized as having large pores (MOF-5 and ZIF-8), small pores (MOF-508 and MIL-53) and pores featuring open metal sites (HKUST-1 and MOF-505). It was observed that the MOFs with large pores did not show good

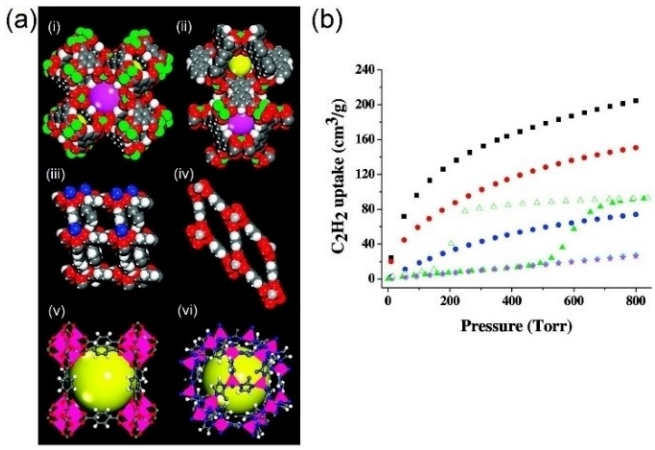

Figure 1. (i) Single-crystal X-ray structures of (a) HKUST-1, (b) MOF-505, (c) MOF-508, (d) MIL-53, (e) MOF-5, and (f) ZIF-8, showing open Cu^{2+} sites (green), 3D frameworks and corresponding pore/cage sizes; and (ii) acetylene adsorption isotherms of microporous MOFs at 295 K (MOF-508 at 290 K). HKUST-1 (black); MOF-505 (red); MOF-508 (green); MIL-53 (blue); MOF-5 (cyan); and ZIF-8 (magenta). Adapted from Ref. [10]. Copyright (2009), with permission from American Chemical Society.

acetylene uptake capacities; the ones having small pores displayed a moderate uptake; and those with open metal Cu^{2+} sites demonstrated significant uptake amounts of 201 $cm^3 g^{-1}$ (HKUST-1) and 148 $cm^3 g^{-1}$ (MOF-505). The neutron powder diffraction studies further established the presence of strong interactions between the open Cu^{2+} sites and the acetylene molecules with 1.67 C_2H_2 per Cu.[10]

Despite numerous MOFs reported thereafter, HKUST-1 remained the best performing material for acetylene storage for

Dr. Gaurav Verma obtained his Ph.D. from the University of South Florida in 2020 under the supervision of Prof. Shengqian Ma. Currently he is working as a Postdoctoral Research Fellow in the group of Prof. Shengqian Ma at the University of North Texas. His areas of interest include design and synthesis of MOFs for energy, catalysis and separation applications.

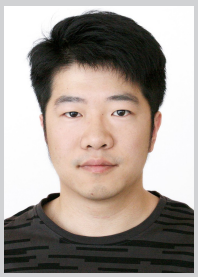

Junyu Ren received his MS from Shandong University in 2017. He is currently a PhD candidate in University of North Texas under the supervision of Prof. Shengqian Ma. His current research interests include the design of functional porous materials for environmental remediation applications.

Dr. Sanjay Kumar obtained his Ph.D degree from Punjabi University, Patiala, India and worked as a UGC Raman Postdoctoral Fellow with Prof. Shengqian Ma from November 2014 to March 2016 at the University of South Florida. He is currently working as an Assistant Professor in Chemistry at Multani Mal Modi College, Patiala, India. His research interests include synthetic organic chemistry, porous materials with a focus on design and synthesis of MOFs, and the applications of MOFs for catalysis, separation, and gas storage.

Prof. Shengqian Ma obtained his B.S. degree from Jilin University, China in 2003, and graduated from Miami University (Ohio) with a Ph.D. degree in 2008. After finishing two-year Director's Postdoctoral Fellowship at Argonne National Laboratory, he joined the Department of Chemistry at University of South Florida (USF) as an Assistant Professor in August 2010. He was promoted to an Associate Professor with early tenure in 2015 and to a Full Professor in 2018. In August 2020, he joined the Department of Chemistry at University of North Texas (UNT) as the Robert A. Welch Chair in Chemistry.

a long time until it was surpassed by FJI–H8 exploiting the similar concept of optimal pore size and rich open metal sites. Pang and coworkers employed dicopper(II) paddlewheel secondary building units (SBUs) and an octacarboxylate linker 3,3′,5,5′-tetra(3,5-dicarboxyphenyl)-4,4′-dimethoxy-biphenyl (H_8tddb) to generate the MOF FJI–H8 $[Cu_4(tddb)\cdot(H_2O)_4]_n\cdot(solvent)_x$ featuring three different types of polyhedral nanocages (Figure 2). As expected, due to the presence of open metal sites and moderate pores, the FJI–H8 displayed a very high acetylene uptake capacity of 224 cm^3 (STP) g^{-1}. Moreover, upon increasing the temperature to 308 K, it could still retain an uptake amount of 200 $cm^3 g^{-1}$; and accounted for only a minimal loss of 3.8% after five cycles of acetylene adsorption/desorption at 295 K (Figure 3), making it an excellent material for practical applications.[11] To explore the effect of linker functionalization and gain a better understanding of the mechanism of gas-sorbate interactions, Schroder and coworkers synthesized a tetra-amide functionalized MOF MFM-188 that exhibited an exceptionally high acetylene uptake of 232 cm^3 (STP) g^{-1}. The cooperative binding effect from the open Cu^{2+} sites and the free amide groups (Figure 4), augmented by the suitable well-defined pore windows led to this record high acetylene uptake as confirmed by neutron diffraction and inelastic neutron scattering studies.[12]

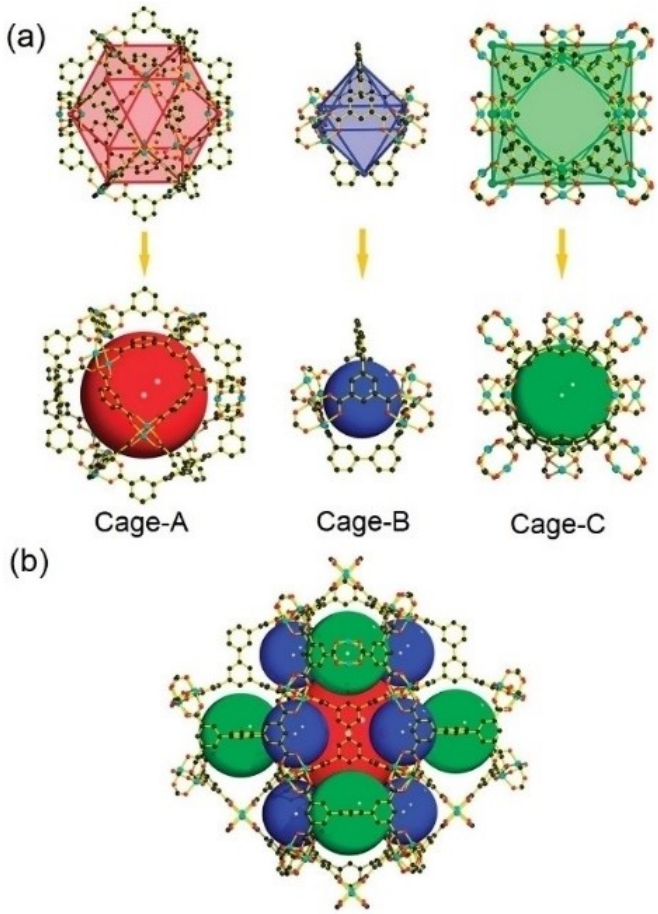

Figure 2. (a) Three types of polyhedral nanocages observed in **FJI-H8**, that is, one regular cuboctahedral cage (Cage-A), one distorted octahedral cage (Cage-B) and one distorted cuboctahedral cage (Cage-C). (b) Combination of the three types of polyhedral nanocages. Reproduced from Ref. [11]. Copyright (2015), with permission from Springer Nature.

A strategy to strengthen the binding interactions for enhanced acetylene uptake is the use of flexible MOFs that can undergo pore-structure adjustment to allow for better accommodation of the adsorbate. Majority of the MOFs studied for acetylene storage comprise of rigid frameworks that show a reduction in the binding affinity after the strongest binding sites get occupied. Flexible frameworks on the other hand, can show an induced fit behavior whereby the guest molecules can induce a progressive contraction of the network leading to a close-packed fitting and stronger host-guest interactions.

Zeng et al. utilized the flexible $[Zn_3(OH)_2(btca)_2]$ (JNU-1, H_2btca: benzotriazole-5-carboxylic acid) for acetylene storage that displayed an induced fit behavior owing to its framework flexibility, appropriate pore geometry and the cooperative action of the open metal sites. As expected, the adsorption enthalpy increased with an increase in the acetylene loading giving a maximum obtained Q_{st} value (at 2 mmol loading) of 47.6 kJ mol^{-1}. The in situ XRD analysis coupled with theoretical modeling revealed a cooperative simultaneous binding of one acetylene molecule to two open Zn(II) centers, and a breathing of the framework leading to superior guest-host and guest-guest interactions (Figure 5).[13]

More recently, Zaworotko and coworkers reported a flexible square lattice coordination network sql-1-Cu-BF_4 [Cu(4,4′-bipyr-

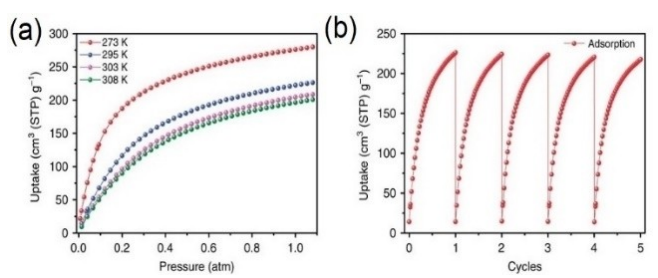

Figure 3. (a) C_2H_2 adsorption isotherms of **FJI-H8** at 273, 295, 303 and 308 K. (b) Cycles of C_2H_2 adsorption for **FJI-H8** at 295 K. Reproduced Ref. [11]. Copyright (2015), with permission from Springer Nature.

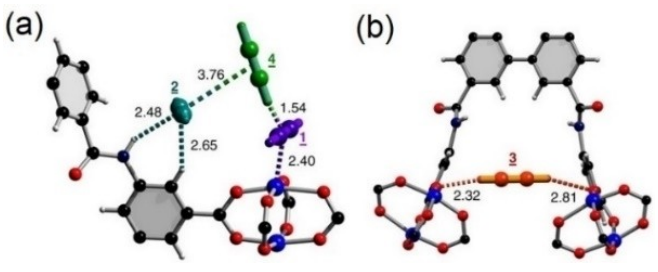

Figure 4. View of the cooperative binding of adsorbed C_2H_2 molecules at site **1, 2, 4** (a) and at site **3** (b). C, black; O, red; H, white; N, blue; Cu, blue. Reproduced from Ref. [12]. Copyright (2017), with permission from Springer Nature.

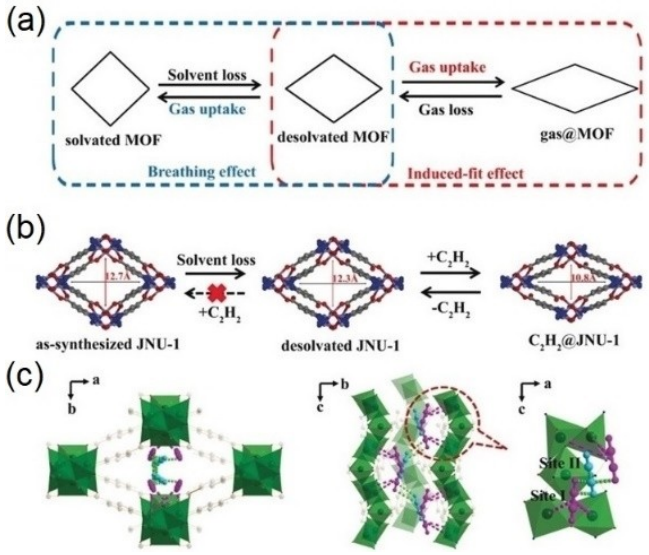

Figure 5. a) Schematic comparison of the breathing and induced-fit effect showing the change in the channel geometry (expansion or shrinkage) upon gas uptake. b) Illustration of the induced-fit behavior in JNU-1. Note the continuous channel shrinkage (guests were omitted for clarity). c) Single-crystal structure of C_2H_2@JNU-1 with observed C_2H_2 molecules on site I (pink) and site II (blue). Reproduced from Ref. [13].

idine)$_2$(BF$_4$)$_2$]$_n$ that undergoes a temperature dependent transition from a nonporous closed form to four open porous phases upon induction by acetylene. The precursor was commercially available and upon heating at 373 K under vacuum generated the nonporous sql-1-Cu-BF$_4$. The acetylene adsorption isotherms measured to 115 kPa at 273 and 298 K displayed two steps with a saturation uptake of 41 cm^3 g^{-1} at the first step and 82 cm^3 g^{-1} on the second. For the isotherms collected between 200–230 K, a third step having a 245 cm^3 g^{-1} adsorption amount was seen; and at 195 K a fourth step emerged around 100 kPa with an uptake capacity of 325 cm^3 g^{-1}. Strong adsorbate-adsorbate (C–H–C≡C) and adsorbate-adsorbent (C–H–F and C≡C-π) interactions were observed with an intrinsic heat management during the adsorption and desorption owing to contraction/expansion of the adjacent layers. Furthermore, the material had a slightly superior working capacity at 288 K over a safer pressure range (1–3.5 vs 1–15 bar).[14]

Another promising strategy for tuning the binding sites to bring about more efficient interactions and better acetylene capture is the pore space partition (PSP) that as the name suggests, partitions the pore space of MOFs into multiple domains by the use of partitioning agents (PPAs). Wang et al. utilized this PSP strategy to partition the MIL-88 type acs frameworks via in situ generated 4,4′-dipyridylsulfide (dps) ligands, leading to partitioned acs (pacs) crystalline porous materials (CPM) shown in Figure 6. In the resultant framework, one-third of the open metal sites remained unoccupied while the remaining two-thirds were used for pore-space partition. The dps-VCo-BDC MOF exhibited exceptionally high acetylene uptake of 330 cm^3 g^{-1} at 273 K and 234 cm^3 g^{-1} at 298 K.

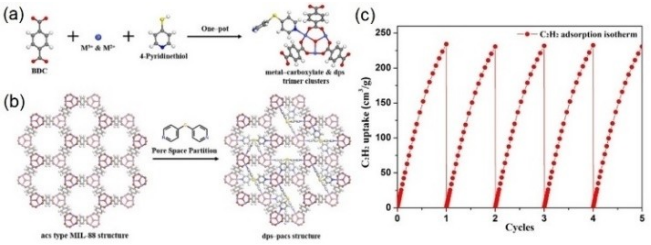

Figure 6. a) dps-assisted metal-carboxylate trimer formation through coordination bonds and in situ desulfation coupling of 4-pyridinethiol, b) Pore space partition by dps and c) Cycles of C_2H_2 adsorption-desorption for dps-VCo-BDC at 298 K. Adapted from Ref. [15].

Moreover, it could be recycled for five acetylene adsorption/desorption cycles at 298 K without any loss in the uptake capacity.[15]

The nanotraps comprising of multiple adsorption sites can also lead to stronger binding affinity and highly selective recognition capability for the targeted guest adsorbates. Recently, our group developed an ultra-strong acetylene nanotrap ATC–Cu ([Cu$_2$(ATC)], ATC: 1,3,5,7-adamantane tetracarboxylate) built from Cu paddlewheel SBUs and the ATC linker; with rectangular channels of dimensions 4.43 Å × 5.39 Å. The complementary effect of oppositely adjacent unsaturated metal sites and aliphatic hydrocarbon cavities led to record high uptakes of 2.54 and 2.1 mmol g^{-1} at 10^{-3} and 10^{-2} bar (298 K), respectively. The uptake at 1 bar reached 5.01 mmol g^{-1} and an exceptionally high Q_{st} value of 79.1 kJ mol^{-1} was obtained, entailing the presence of very strong binding interactions between acetylene molecules and the MOF. The single crystal XRD studies on acetylene loaded MOF indicated the trapping of acetylene molecules in the nanotraps at very low pressure, followed by filling of the aliphatic hydrocarbon cavities upon increasing the pressure (Figure 7).[16] Moreover, the material could also show

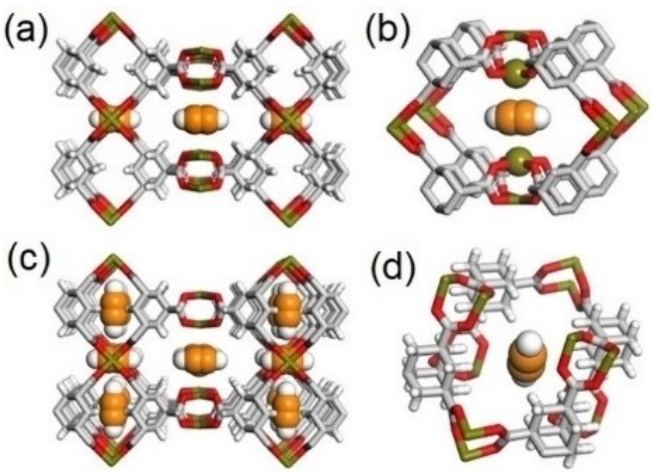

Figure 7. The SCXRD determined the location of C_2H_2 a) in the framework of ATC–Cu and b) on the Site I at 1 × 10^{-4} bar, and in the framework of ATC–Cu and c) on the Site II d) at 1 bar. Reproduced from Ref. [16].

high selectivity for acetylene separation, which has been discussed with other materials in the following sections.

3. Acetylene Separation using MOFs

3.1. Separation of Acetylene from Carbon dioxide

The Kitagawa group first reported the C_2H_2/CO_2 separation using the $[Cu_2(pzdc)_2(pyz)]$ MOF whereby the maximum amount of C_2H_2 adsorbed was 26 times that of CO_2. A higher Q_{st} value for acetylene compared to carbon dioxide was observed, indicating better interaction of the acetylene molecules with the framework.[2]

The hybrid ultramicroporous materials (HUMs) are a subclass of MOFs featuring narrow pore sizes and pillars comprising of inorganic anions (SiF_6^{2-}, $Cr_2O_7^{2-}$, and MoO_4^{2-}) that lead to highly electrostatic pore surfaces. These can be tuned to afford strong binding interactions with one adsorbate over the other. Zaworotko et al. have pioneered this field of HUMs and in 2016 reported TIFSIX-**2**-Cu-i (**2**: 1,2-bis(4-pyridyl)acetylene, i: interpenetrated) that showed a higher C_2H_2 uptake compared to CO_2 at low loading and a selectivity of 6.5 at 298 K and 1 bar for a 2:1 mixture. Interestingly, analogous SIFSIX-3-Ni with similar pore size and chemistry exhibited high CO_2/C_2H_2 selectivity and this inverse selectivity could be attributed to the size and geometry of the binding site.[17]

Ye et al. utilized the pore-space partition strategy to generate FJU-90 from FJU-88 by using a triangular linker 2,4,6-tris(4-pyridyl)pyridine (Tripp) as the partitioning agent. The pore apertures were reduced from 12.0 Å × 9.4 Å in FJU-88 to 5.4 Å × 5.1 Å in FJU-90 resulting in stronger electrostatic and hydrogen bonding interactions between the framework and acetylene. A high Q_{st} value of 25.1 kJ mol^{-1} was observed for acetylene compared to CO_2 (20.7 kJ mol^{-1}) with an IAST selectivity of 4.3 for an equimolar C_2H_2/CO_2 mixture at 298 K. The breakthrough experiments further revealed a high dynamic C_2H_2 capture productivity of 1.87 mol kg^{-1} with excellent recyclability over five cycles (Figure 8).[18]

Zhai and coworkers also adopted the PSP approach to partition the MIL-88 type acs networks into small finite segments having pore sizes of widths 4.5–8.1 Å (SNNU-26-M, SNNU-27-M, SNNU-28-M and SNNU-29-M) by using ditopic linkers BDC (1,4-terephthalic acid), TAZBC (4-(1H-tetrazol-5-yl) benzoic acid), 2,6-NDC (naphthalene-2,6-dicarboxylic acid), BDT (1,4-benzeneditetrazole); and 2,4,6-tri(4-pyridinyl)-1-pyridine (TPP) as the partitioning agent. The presence of tetrazole groups as hydrogen-bonding acceptors, suitable pore sizes and robust frameworks; the materials exhibited high acetylene uptake capacity, excellent C_2H_2/CO_2 selectivity and good stability. The optimized SNNU-27-Fe displayed an acetylene uptake capacity of 182.4 cm^3 g^{-1} and record dynamic breakthrough time of up to 91 min g^{-1} for C_2H_2/CO_2 separation under ambient conditions.[19]

The multivariate MOFs (MTV-MOFs) are another class of materials that have emerged recently, comprising of multiple linkers having various functionalities in a single framework that offer enormous structural diversity and synergistic effects. Zhou and coworkers obtained 25 different MOFs from the parent UPC-200 comprising of varied pore size, pore environments and functional groups. The optimized UPC200(Al)-F-BIM featuring dangling benzimidazole ligands and pores lined with fluorine functional groups to give a high C_2H_2/CO_2 uptake ratio of 2.6 with a selectivity of 3.15 at 298 K and 1 bar. Moreover, the material exhibited a low Q_{st} between 18.9 and 20.5 kJ mol^{-1} making it an economically viable material with low regeneration energy.[20]

The similar kinetic diameters and identical molecular shape/size of acetylene and carbon dioxide make it difficult and challenging to achieve high selectivity and separation for the C_2H_2/CO_2 mixtures. A tradeoff exists between the uptake capacity and selectivity, and a high density of functional sites with narrow pores (like HUMs) could offer effective separation whilst retaining high uptake capacities. Taking inspiration, Chen and coworkers reported a mixed metal organic framework FeNi–M′MOF: $[Fe(pyz)Ni(CN)_4]$(pyz = pyrazine), whereby the acetylene molecules could bind with the organic moieties by π-π stacking and open Ni sites by multiple intermolecular interactions; whereas the CO_2 molecules were distributed only on the open Ni sites via weaker interactions. The material thus displayed an excellent selectivity of 24 at 298 K and 1 bar for a 50:50 C_2H_2/CO_2 mixture and a high C_2H_2 capture amount of 4.54 mol L^{-1} by simulated column breakthrough experiments (Figure 9).[21]

In order to implement the porous materials for practical industrial applications, the stability of the adsorbent under harsh environments is must whilst retaining their porosities and

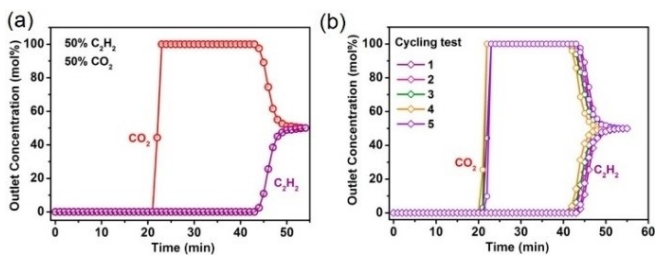

Figure 8. Experimental breakthrough curves for (a) an equimolar C_2H_2/CO_2 mixture and (b) a cycling test of the equimolar C_2H_2/CO_2 mixture in a packed column with **FJU-90 a** at 298 K and 1 bar. Reproduced from Ref. [18]. Copyright (2019), with permission from American Chemical Society.

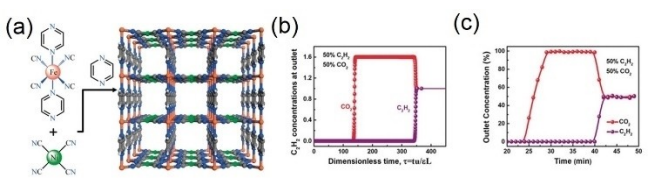

Figure 9. a) The crystal structure of **FeNi-M′MOF** viewed along the *a*/*b* axis, b) Transient breakthrough simulations for separation of equimolar C_2H_2/CO_2 mixture using **FeNi-M′MOF** at 298 K, with a partial pressure of 50 kPa for each, and c) Experiment breakthrough curves for equimolar C_2H_2/CO_2 mixture in a packed column with **FeNi-M′MOF** at 298 K and 1 bar. Adapted from Ref. [21].

uptake capacities. Pei et al. synthesized a chemically stable Hofmann-type MOF ZJU-74a that consisted of adjacent opposite coordinatively unsaturated metal centers and high-density cyanide groups leading to a sandwich-like binding environment for the acetylene molecules (Figure 10). The material featured a record high acetylene uptake capacity of 49 $cm^3 g^{-1}$ at low pressure (0.01 bar) and 298 K, along with a benchmark C_2H_2/CO_2 selectivity of 36.5. Moreover, it displayed high chemical stability in aqueous and acid-base environments evident from the PXRD patterns and could mostly retain its surface area and acetylene uptake capacities.[22]

The ATC–Cu nanotrap featured by our group exhibited similar oppositely adjacent coordinatively unsaturated metal centers with additional aliphatic hydrocarbon cavities that led to a benchmark C_2H_2/CO_2 selectivity of 53.6 at 298 K and 1 bar, surpassing ZJU-74a. The breakthrough experiments further revealed that a complete separation of acetylene from 1:1 C_2H_2/CO_2 mixtures could be realized.[16]

More recently, we reported a strategy of window space-directed assembly (WSDA) for molecular sieving and enhancing the host-guest interactions, whereby ultramicropore structures can be obtained by partial blocking of the windows of the large cage. The resultant ST-sod-MOFs $[M_3(OH/O)(H_2O)(btc)_2(tpt)_{2/3}$ (btc: 1,3,5-benzenetricarboxylate, tpt: 2,4,6-tri(4-pyridyl)-1,3,5-triazine, and M_3: Co_3,Ni_3 or Co_2Ti) consisted of the paired tpt ligands acting as the WSD agents (Figure 11). The ST-sod-Co/Ti exhibited the highest BET surface area among the three MOFs and a decent selectivity value of 2.66 at 0.01 bar and 298 K for an equimolar C_2H_2/CO_2, which decreased to 1.65 at 1 bar. The breakthrough experiments revealed an effective capture of acetylene from the C_2H_2/CO_2 mixture and a good stability and recyclability for four cycles. Despite showing a lower selectivity, this work provides a new approach for effective acetylene capture and separation by WSDA.[23]

Zhang and coworkers reported a MOF Cu^I@UiO-66-$(COOH)_2$ featuring Cu^I sites capable of interacting with acetylene molecules to generate copper(I)-alkynyl π-complex (Figure 12). These anchored Cu^I sites led to the adsorption of a large amount of C_2H_2 and a drastically high C_2H_2/CO_2 selectivity value of 185 at ambient conditions, outperforming the previously reported benchmark materials. The excellent selectivity performance was further evidenced by breakthrough experiments and the theoretical calculations further suggested the presence of π-complexation as the main reason for this ultra-strong binding affinity and record selectivity (Figure 13). Thus, this work provides new avenues for use post-grafted materials on the framework to attain strong interactions leading to ultrahigh C_2H_2/CO_2 separation performance.[24]

Another strategy of adsorption site selective occupation was very recently reported by Zhao and coworkers whereby they employed the difference in orientation of acetylene and

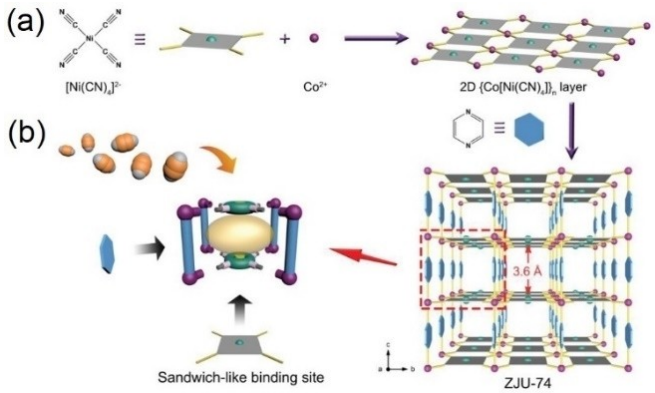

Figure 10. Structure description of ZJU-74. a) Construction of 2D $Co[Ni(CN)_4]_n$ layers with pyz ligands to form 3D Hofmann-type networks in ZJU-74. b) Schematic illustration of the sandwich-like binding site in ZJU-74 for C_2H_2 capture. Reproduced from Ref. [22].

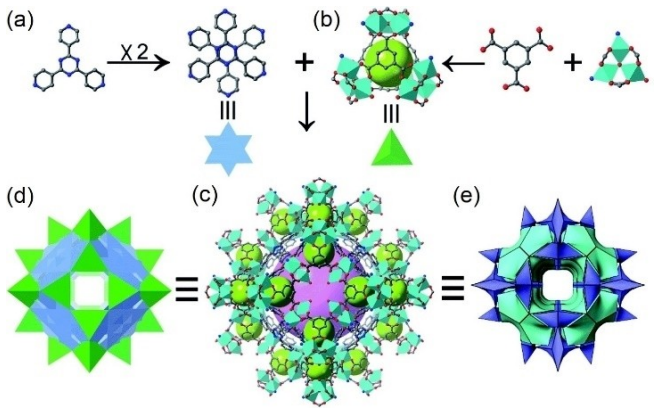

Figure 11. Schematic of the ST-**sod**-MOF assembly process using ST-**sod**-Co as an example. (a) A pair of staggered tpt ligands were formed *via* π-π stacking interactions. (b) The ST building block was composed of classic cobalt trimers $[Co_3(OH)(COO)_6]$ and btc ligands. (c) A β-cavity mesoporous cage in ST-**sod**-Co. (d) ST-**sod**-Co interconnected *via* a **sod** framework with closed hexagonal windows when the STs are considered as nodes. (e) The corresponding tiling model in ST-**sod**-Co. Reproduced from Ref. [23]. Copyright (2021), with permission from Royal society of Chemistry.

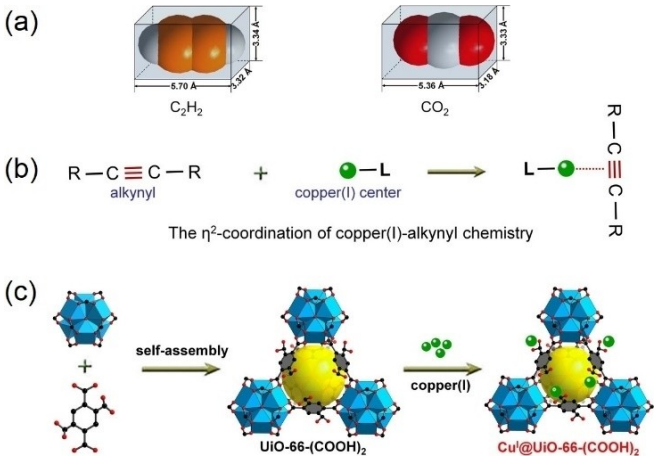

Figure 12. a) Comparison of molecular size difference of C_2H_2 and CO_2; b) The π-coordination chemistry between alkynes and copper(I) ions; c) The self-assembly of 2-connected linker and 12-connected Zr-cluster to form 3D *fcu*-topology framework of UiO-66-$(COOH)_2$, and copper(I) ions can be anchored through the coordination with bare carboxylate groups. Reproduced from Ref. [24].

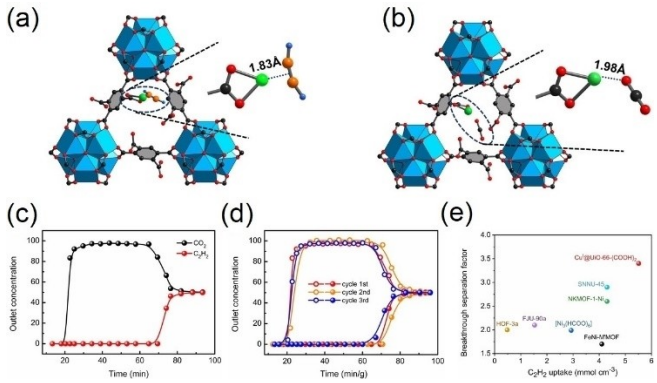

Figure 13. Comparison of the preferential C_2H_2 (a) and CO_2 (b) binding sites and models observed by theoretical calculations. c) Experimental breakthrough curves of Cu^I@UiO-66-$(COOH)_2$ for the C_2H_2/CO_2 (50/50) separation at 298 K with a constant flow rate of 2 mL min^{-1}; d) Multiple cycles of breakthrough tests of Cu^I@UiO-66-$(COOH)_2$ for C_2H_2/CO_2 separation; e) Comparison of the breakthrough separation factor and C_2H_2 uptake among top performing porous materials at equal molar C_2H_2/CO_2 separation. Reproduced from Ref. [24].

CO_2 for the corresponding sieving, separation and purification. The CO_2 molecules adapt an end-on orientation aligning themselves with the geometry of the channel whereas the acetylene molecules prefer a side-on orientation. Thus, selectively filling up the CO_2 adsorption sites whilst leaving the acetylene binding sites intact could lead to an exclusive binding of C_2H_2. Keeping this in mind, amine-functionalized CPL-1 [Cu_2(pzdc)$_2$pyz-NH_2], a derivative of the first acetylene storage MOF reported by Kitagawa was synthesized. Since the CO_2 adsorption sites were now occupied by the amino groups on the pillars, a significantly lower amount of CO_2 was adsorbed onto the framework leading to a high C_2H_2/CO_2 selectivity of 119 at ambient conditions.[25]

3.2. Separation of Acetylene from Methane, Ethylene and Other Hydrocarbons

The early examples for acetylene separation included the magnesium/manganese formates, Cu(BDC-OH), M'MOF-2/3, UTSA-33, RPM3-Zn etc. that displayed good selectivity over small hydrocarbons such as methane and ethylene. Since then, numerous examples of porous materials have been reported for separation over propane/propylene and even ternary or quaternary mixtures of these hydrocarbons.

Cui et al. optimized the pore size and pore chemistry to generate the SIFSIX-2-Cu-i and SIFSIX-1-Cu that exhibited excellent selectivity for the capture of acetylene and its separation from ethylene. The weakly basic SiF_6^{2-} sites lining the pore walls afforded stronger binding interactions with the weakly acidic acetylene molecules leading to C_2H_2/C_2H_4 selectivities of 39.7 to 44.8 for SIFSIX-2-Cu-i and 7.1 to 10.6 for SISIX-1-Cu.[26]

Guo and coworkers utilized a diarylethene MOF as a temperature and light responsive switch for C_2H_2/C_2H_4 separation. The presence of the unique control of this C_2H_2/C_2H_4 selectivity was attributed to the guest discriminatory gate-opening effect arising from the diarylethene unit. A high selectivity of 47.1 was achieved at 195 K for an equimolar mixture.[27]

The ultramicroporous NKMOF-1-M with the structural formula Cu[M(pdt)$_2$] (M: Cu, Ni; pdt: pyrazine-2,3-dithiol) featuring strong binding interactions and small pores were also explored for C_2H_2/CH_4 and C_2H_2/C_2H_4 separation. Ultrahigh IAST adsorption selectivities of 1272.6, 346.5, 6409.1, and 4949.2 were obtained for C_2H_2/C_2H_4 (1/99), C_2H_2/C_2H_4 (1/9), C_2H_2/CH_4 (1/1), and C_2H_2/CH_4 (2/1), respectively in the case of NKMOF-1-Ni at ambient conditions (Figure 14). A new type of binding site for C_2H_2 was identified from the modeling and in situ SCXRD studies, with a Q_{st} value of 53.9 kJ mol^{-1} obtained for NKMOF—Ni-1 at that site.[28]

A closo-dodecaborate cluster $[B_{12}H_{12}]^{2-}$ based MOF BSF-1 assembled from 1,2-bis(4 pyridyl)acetylene (bpa) and copper(II) dodecaborate was also explored for C_2H_2/CH_4 and C_2H_2/C_2H_4 separations (Figure 15). The material had a structure similar to the HUMs and featured nonclassical B—H···M and B—H$^{\delta-}$···H$^{\delta+}$—C interactions. The selectivity values obtained at 298 K and 1 bar were 46.9 and 2.3 for C_2H_2/CH_4 and C_2H_2/C_2H_4 respectively.[29]

Li et al. reported a nearly ideal molecular sieve for the separation of acetylene from ethylene. The SIFSIX-14-Cu-i (or UTSA-200) composed of 4,4'-azopyridine linkers and $CuSiF_6$ units featured the optimal pore size of 3.4 Å and very strong interactions with the C_2H_2 molecules evident from the very high static binding energy ΔE of 56 kJ mol^{-1}. The material exhibited a benchmark acetylene uptake capacity of 58 cm^3 cm^{-3} at 0.01 bar and 298 K; and negligible C_2H_4 uptake below 0.2 bar. An extraordinarily high selectivity of over 6000 at 298 K and 1 bar was observed for 1:99 (v/v) mixture of C_2H_2:C_2H_4. The breakthrough curves revealed a record purification capacity of the UTSA-200 to remove trace C_2H_2 from C_2H_4, generating highly pure (99.9999%) C_2H_4. Moreover, the UTSA-200 showed no change in the breakthrough times over 12 cycles and an

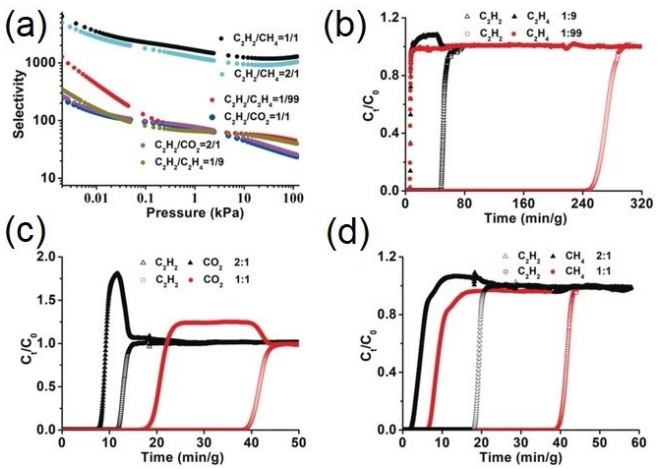

Figure 14. a) IAST adsorption selectivities and b)–d) breakthrough curves of various C_2H_2 gas mixtures at 298 K for **NKMOF-1-Ni**. Reproduced from Ref. [28].

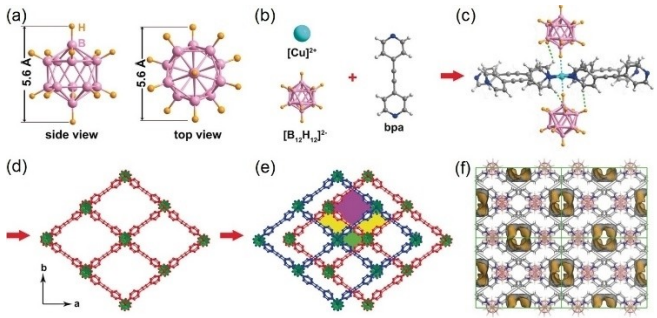

Figure 15. Supramolecular assembly and structure of BSF-1: a) structure of the $[B_{12}H_{12}]^{2-}$ dianion; b) starting materials used for the synthesis of BSF-1; c) interactions between Cu^{II}, $[B_{12}H_{12}]^{2-}$, and bpa, d) Constructed **pcu** network pillared by $[B_{12}H_{12}]^{2-}$, with the green icosahedron representing the dodecaborate pillar. e) Offset interpenetration of two independent **pcu** networks leads to three distinct channels. f) The void space of BSF-1 indicates only the largest channel is available for guests. Reproduced from Ref. [29].

exceptional stability after multiple breakthrough cycles, confirmed by the PXRD of the resultant samples.[30]

ZJU-280, a water stable SIFSIX-type MOF was also utilized by Qian and coworkers for the separation of acetylene from ethylene as well as carbon dioxide. The $[Cu(TPB)SiF_6]_n$ was constructed from $CuSiF_6$ and a four connected N-based linker 1,2,4,5-tetra(pyridin-4-yl)benzene (TPB) with rhombic pores and *fsc* topology, unlike the square pores and *pcu* topology found in the typical SIFSIX materials. High C_2H_2/C_2H_4 selectivities of 44.5 and 33.0 were observed for 1/99 and 50/50 gas mixtures repectively, at 296 K and 1 bar. Furthermore, the material could also exhibit high C_2H_2/CO_2 selectivity of 18.1 for an equimolar mixture and a negligible loss in the separation performance over multiple breakthrough cycles. The high separation performance could be attributed to the rhombic pores and highly strong interactions between the functional pore surfaces and the acetylene molecules.[31]

Compared to the binary mixture separation, the ternary separations are significantly more challenging, often requiring use of multiple adsorbents in different stages. Flexible MOFs can be highly promising in this regard as a single adsorbent for multiple has separations via regulation of the gate opening pressure. Chen and coworkers utilized the flexible NTU-65 for separation of $C_2H_4/C_2H_2/CO_2$ mixture whereby at 263 K, the MOF displayed high uptake capacities of 86.3 $cm^3 g^{-1}$ for C_2H_2 and 79.5 $cm^3 g^{-1}$ for CO_2, but only a negligible amount (2.2 $cm^3 g^{-1}$) of C_2H_4. Thus, high purity polymer grade ethylene could be obtained in a single breakthrough cycle. Furthermore, the material exhibited stability under aqueous and acidic/basic environments, making it a promising material for practical separations.[32]

Zhang et al. explored the HUMs for quaternary separation of a $C_2H_2/C_2H_4/C_3H_4/C_3H_6$ mixture whereby the alkynes acetylene and propyne could be selectively removed using the anion pillared ZU-16-Co. A high C_2H_2 uptake of 1.4 and 4.18 mmol g^{-1} was observed at 0.01 bar and 1 bar respectively and the breakthrough tests for quaternary $C_3H_4/C_2H_2/C_3H_6/C_2H_4$ (0.5/0.5/49.5/49.5) mixture indicated the retention of C_2H_2 and C_3H_4 up to 17 and 58 min, respectively. This performance was attributed to the contracted pore size and judiciously extended cell dimension.[33]

3.3. Inverse CO_2/C_2H_2 separation

Another strategy is to capture the CO_2 instead of acetylene, leading to high purity acetylene streams. This is particularly helpful as CO_2 is the main contaminant in acetylene, however the materials exhibiting inverse CO_2/C_2H_2 selectivity are rare in the literature. Zhao and coworkers utilized the strategy of combining a perfluorinated aromatic spacer TFBDC (tetrafluoroterephthalate) with Ce^{IV} featuring unoccupied 4f orbitals to generate Ce^{IV}-MIL-140-4F with optimal pore chemistry and charge transfer effects for inverse CO_2/C_2H_2 separation. The excellent selectivity values of 9.5 at 298 K and 41 at 273 K were obtained for a 1:2 CO_2/C_2H_2 mixture (Figure 16). Furthermore, the CO_2 Q_{st} value of 39.5 kJ mol-1 was much higher than that for acetylene (27.4 kJ mol^{-1}).[34]

Yang and coworkers reported the bifunctional MOF [Co-(HL^{dc})]·1.5MeOH·dioxane featuring both free acidic carboxylic and free basic pyridyl functionalities within the pores that displayed unusually selective adsorption of CO_2 over C_2H_2 upon desolvation. The CO_2 uptake isotherms at 195 K showed a phase transition from the narrow pore (***np***) to the large pore (***lp***) form leading to an uptake capacity of 240 $cm^3 g^{-1}$, much higher compared to that of C_2H_2 (140 $cm^3 g^{-1}$) and CH_4 (115 $cm^3 g^{-1}$), with the C_2H_2/CO_2 uptake ratio of 0.72:1 at 0.01 bar and 0.58:1 at 1 bar. The strong CO_2-framework interactions led to the phase transition and the high uptake capacity, further confirmed by the in-situ powder X-ray diffraction and GCMC simulations.[35]

Li et al. also synthesized two γ-cyclodextrin (CD) based MOFs, CD-MOF-1 $[K_2(C_{48}H_{80}O_{40})(OH)_2]$ and CD-MOF-2 $[Rb_2(C_{48}H_{80}O_{40})(OH)_2]$ that displayed high CO_2 adsorption capaci-

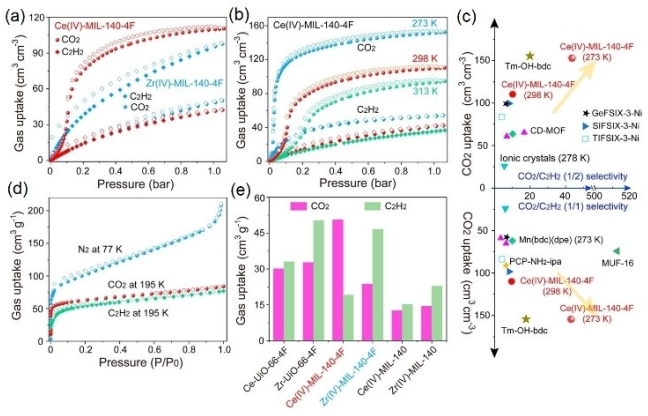

Figure 16. a) CO_2 and C_2H_2 isotherms of Ce^{IV}- and Zr^{IV}-MIL-140-4F collected at 298 K. b) CO_2 and C_2H_2 isotherms of Ce^{IV}-MIL-140-4F collected at different temperatures. c) Comparison of the best-performing materials for CO_2/C_2H_2 separation. d) CO_2 and C_2H_2 isotherms at 195 K and N_2 isotherm at 77 K of Ce^{IV}-MIL-140-4F. e) CO_2 and C_2H_2 uptakes of different materials at 298 K. Reproduced from Ref. [34].

ties and a benchmark CO_2/C_2H_2 selectivity of 118.7 (1 : 2, v/v) for CDMOF-2 at room temperature. The inversion in the selectivity was attributed to the weakly nucleophilic free primary and secondary hydroxyl groups on the γ-CD that could reversibly interact with CO_2.[36]

4. Conclusions

Acetylene storage and separation has come to the fore and become a prominent area of research, with more than 70 publications reported in just the last year and a half. MOFs have heralded the new developments in this application, balancing the trade-off between the uptake capacity and selectivity by designing small pores and highly functionalized pore environments for strong binding with the acetylene adsorbate. Moreover, strategies such as pore space partition, window space directed assembly and inverse CO_2/C_2H_2 have led to benchmark acetylene uptake capacities and selectivities over CO_2, CH_4, C_2H_6 and other hydrocarbons. The stability of the framework and breakthrough tests are vital for the practical development of these materials. An increasing number of studies are addressing these factors, but more work needs to be done in this direction to achieve an industrial scale realization of these materials. Although some of these materials have shown good recyclability over breakthrough cycles, the performance needs to be assessed over thousands of cycles and breakthough experiments be a must for every material for its evaluation in the practical usage. Furthermore, processing of these materials into membranes and study of the uptake performance after the MOF processing needs to be looked into as well. Currently, MOFs can lose up to 25% of their performance after processing. Strategies to overcome the loss of crystallinity and maintain the storage and separation performance will be the challenges going forward in this direction.

Acknowledgements

The authors acknowledge the Robert A. Welch Foundation (B-0027) for financial support of this work.

Conflict of Interest

The authors declare no conflict of interest.

Keywords: Acetylene separation · Acetylene storage · Binding interactions · Metal-organic frameworks · Selectivity

[1] a) R. J. Tedeschi, in *Encyclopedia of Physical Science and Technology (Third Edition)* (Ed.: R. A. Meyers), Academic Press, New York, **2003**, pp. 55–89; b) H. Schobert, *Chem. Rev.* **2014**, *114*, 1743–1760.
[2] R. Matsuda, R. Kitaura, S. Kitagawa, Y. Kubota, R. V. Belosludov, T. C. Kobayashi, H. Sakamoto, T. Chiba, M. Takata, Y. Kawazoe, Y. Mita, *Nature* **2005**, *436*, 238–241.
[3] a) W. Fan, S. B. Peh, Z. Zhang, H. Yuan, Z. Yang, Y. Wang, K. Chai, D. Sun, D. Zhao, *Angew. Chem. Int. Ed.* **2021**, https://doi.org/10.1002/anie.202102585; b) J. P. Zhang, X. M. Chen, *J. Am. Chem. Soc.* **2009**, *131*, 5516–5521; c) W. Fan, S. B. Peh, Z. Zhang, H. Yuan, Z. Yang, Y. Wang, K. Chai, D. Sun, D. Zhao, *Angew. Chem. Int. Ed.* **2021**, *60*, 17338–17343.
[4] a) S. H. Zhang, M. K. Taylor, L. C. Jiang, H. Ren, G. S. Zhu, *Chem. Eur. J.* **2020**, *26*, 3205–3221; b) L. Li, H. Ma, J. Zhang, E. Zhao, J. Hao, H. Huang, H. Li, P. Li, X. Gu, B. Z. Tang, *J. Am. Chem. Soc.* **2021**, *143*, 3856–3864; c) M. M. Deegan, M. R. Dworzak, A. J. Gosselin, K. J. Korman, E. D. Bloch, *Chem. Eur. J.* **2021**, *27*, 4531–4547; d) S. Lim, H. Kim, N. Selvapalam, K.-J. Kim, S. J. Cho, G. Seo, K. Kim, *Angew. Chem. Int. Ed.* **2008**, *47*, 3352–3355; *Angew. Chem.* **2008**, *120*, 3400–3403; e) M. A. Little, A. I. Cooper, *Adv. Funct. Mater.* **2020**, *30*, 1909842.
[5] C. D. Charles, E. D. Bloch, *Supramol. Chem.* **2019**, *31*, 508–513.
[6] a) C. Krishnaraj, H. S. Jena, K. Leus, H. M. Freeman, L. G. Benning, P. Van der Voort, *J. Mater. Chem. A* **2019**, *7*, 13188–13196; b) Y. Lu, J. He, Y. L. Chen, H. Wang, Y. F. Zhao, Y. Han, Y. Ding, *Macromol. Rapid Commun.* **2018**, *39*, 1700468.
[7] a) H. C. Zhou, J. R. Long, O. M. Yaghi, *Chem. Rev.* **2012**, *112*, 673–674; b) A. E. Baumann, D. A. Burns, B. Liu, V. S. Thoi, *Commun. Chem.* **2019**, *2*, 86; c) M. J. Kalmutzki, N. Hanikel, O. M. Yaghi, *Sci. Adv.* **2018**, *4*, eaat9180.
[8] a) M. Safaei, M. M. Foroughi, N. Ebrahimpoor, S. Jahani, A. Omidi, M. Khatami, *TrAC Trends Anal. Chem.* **2019**, *118*, 401–425; b) X. Zhang, Z. Chen, X. Liu, S. L. Hanna, X. Wang, R. Taheri-Ledari, A. Maleki, P. Li, O. K. Farha, *Chem. Soc. Rev.* **2020**, *49*, 7406–7427; c) Z. Ji, H. Wang, S. Canossa, S. Wuttke, O. M. Yaghi, *Adv. Funct. Mater.* **2020**, *30*, 2000238; d) A. Kirchon, L. Feng, H. F. Drake, E. A. Joseph, H.-C. Zhou, *Chem. Soc. Rev.* **2018**, *47*, 8611–8638.
[9] a) Y. Li, G. L. Wen, *Eur. J. Inorg. Chem.* **2020**, *2020*, 2303–2311; b) X. P. Fu, Y. L. Wang, Q. Y. Liu, *Dalton Trans.* **2020**, *49*, 16598–16607; c) J. Y. Pei, K. Shao, L. Zhang, H. M. Wen, B. Li, G. D. Qian, *Top. Curr. Chem.* **2019**, *377*, 33; d) R. B. Lin, S. C. Xiang, H. B. Xing, W. Zhou, B. L. Chen, *Coord. Chem. Rev.* **2019**, *378*, 87–103; e) B. R. Barnett, M. I. Gonzalez, J. R. Long, *Trends Chem.* **2019**, *1*, 159–171; f) Y. B. He, F. L. Chen, B. Li, G. D. Qian, W. Zhou, B. L. Chen, *Coord. Chem. Rev.* **2018**, *373*, 167–198; g) K. Adil, Y. Belmabkhout, R. S. Pillai, A. Cadiau, P. M. Bhatt, A. H. Assen, G. Maurin, M. Eddaoudi, *Chem. Soc. Rev.* **2017**, *46*, 3402–3430; h) Y. J. Cui, B. Li, H. J. He, W. Zhou, B. L. Chen, G. D. Qian, *Acc. Chem. Res.* **2016**, *49*, 483–493; i) B. Li, B. L. Chen, in *Lanthanide Metal-Organic Frameworks, Vol. 163* (Ed.: P. Cheng), **2015**, pp. 75–107; j) D. Banerjee, J. Liu, P. K. Thallapally, *Comments Inorg. Chem.* **2015**, *35*, 18–38; k) Y. B. He, W. Zhou, R. Krishna, B. L. Chen, *Chem. Commun.* **2012**, *48*, 11813–11831; l) R. B. Getman, Y. S. Bae, C. E. Wilmer, R. Q. Snurr, *Chem. Rev.* **2012**, *112*, 703–723; m) Z. J. Zhang, S. C. Xiang, B. L. Chen, *CrystEngComm* **2011**, *13*, 5983–5992; n) S. Q. Ma, L. Meng, *Pure and Appl. Chem.* **2011**, *83*, 167–188; o) Z. Bao, G. Chang, H. Xing, R. Krishna, Q. Ren, B. Chen, *Energy Environ. Sci.* **2016**, *9*, 3612–3641.
[10] S. C. Xiang, W. Zhou, J. M. Gallegos, Y. Liu, B. L. Chen, *J. Am. Chem. Soc.* **2009**, *131*, 12415–12419.
[11] J. D. Pang, F. L. Jiang, M. Y. Wu, C. P. Liu, K. Z. Su, W. G. Lu, D. Q. Yuan, M. C. Hong, *Nat. Commun.* **2015**, *6*, 7575.
[12] F. Moreau, I. da Silva, N. H. Al Smail, T. L. Easun, M. Savage, H. G. W. Godfrey, S. F. Parker, P. Manuel, S. H. Yang, M. Schroder, *Nat. Commun.* **2017**, *8*, 14085.
[13] H. Zeng, M. Xie, Y. L. Huang, Y. F. Zhao, X. J. Xie, J. P. Bai, M. Y. Wan, R. Krishna, W. G. Lu, D. Li, *Angew. Chem. Int. Ed.* **2019**, *58*, 8515–8519; *Angew. Chem.* **2019**, *131*, 8603–8607.
[14] S.-Q. Wang, X.-Q. Meng, M. Vandichel, S. Darwish, Z. Chang, X.-H. Bu, M. J. Zaworotko, *ACS Appl. Mater. Interfaces* **2021**, *13*, 23877–23883.
[15] Y. Wang, X. X. Jia, H. J. Yang, Y. X. Wang, X. T. Chen, A. N. Hong, J. P. Li, X. H. Bu, P. Y. Feng, *Angew. Chem. Int. Ed.* **2020**, *59*, 19027–19030; *Angew. Chem.* **2020**, *132*, 19189–19192.
[16] Z. Niu, X. Cui, T. Pham, G. Verma, P. C. Lan, C. Shan, H. Xing, K. A. Forrest, S. Suepaul, B. Space, A. Nafady, A. M. Al-Enizi, S. Ma, *Angew. Chem. Int. Ed.* **2021**, *60*, 5283–5288; *Angew. Chem.* **2021**, *133*, 5343–5348.
[17] K. J. Chen, H. S. Scott, D. G. Madden, T. Pham, A. Kumar, A. Bajpai, M. Lusi, K. A. Forrest, B. Space, J. J. Perry, M. J. Zaworotko, *Chem* **2016**, *1*, 753–765.
[18] Y. X. Ye, Z. L. Ma, R. B. Lin, R. Krishna, W. Zhou, Q. J. Lin, Z. J. Zhang, S. C. Xiang, B. L. Chen, *J. Am. Chem. Soc.* **2019**, *141*, 4130–4136.
[19] Y.-Y. Xue, X.-Y. Bai, J. Zhang, Y. Wang, S.-N. Li, Y.-C. Jiang, M.-C. Hu, Q.-G. Zhai, *Angew. Chem. Int. Ed.* **2021**, *60*, 10122–10128.

[20] W. D. Fan, S. Yuan, W. J. Wang, L. Feng, X. P. Liu, X. R. Zhang, X. Wang, Z. X. Kang, F. N. Dai, D. Q. Yuan, D. F. Sun, H. C. Zhou, *J. Am. Chem. Soc.* **2020**, *142*, 8728–8737.
[21] J. K. Gao, X. F. Qian, R. B. Lin, R. Krishna, H. Wu, W. Zhou, B. L. Chen, *Angew. Chem. Int. Ed.* **2020**, *59*, 4396–4400; *Angew. Chem.* **2020**, *132*, 4426–4430.
[22] J. Pei, K. Shao, J.-X. Wang, H.-M. Wen, Y. Yang, Y. Cui, R. Krishna, B. Li, G. Qian, *Adv. Mater.* **2020**, *32*, 1908275.
[23] L. Zhang, F. Li, J. You, N. Hua, Q. Wang, J. Si, W. Chen, W. Wang, X. Wu, W. Yang, D. Yuan, C. Lu, Y. Liu, A. M. Al-Enizi, A. Nafady, S. Ma, *Chem. Sci.* **2021**, *12*, 5767–5773.
[24] L. Zhang, K. Jiang, L. Yang, L. Li, E. Hu, L. Yang, K. Shao, H. Xing, Y. Cui, Y. Yang, B. Li, B. Chen, G. Qian, *Angew. Chem. Int. Ed.* **2021**, *60*, 15995–16002.
[25] L. Yang, L. Yan, Y. Wang, Z. Liu, J. He, Q. Fu, D. Liu, X. Gu, P. Dai, L. Li, X. Zhao, *Angew. Chem. Int. Ed.* **2021**, *60*, 4570–4574; *Angew. Chem.* **2021**, *133*, 4620–4624.
[26] X. L. Cui, K. J. Chen, H. B. Xing, Q. W. Yang, R. Krishna, Z. B. Bao, H. Wu, W. Zhou, X. L. Dong, Y. Han, B. Li, Q. L. Ren, M. J. Zaworotko, B. L. Chen, *Science* **2016**, *353*, 141–144.
[27] C. B. Fan, L. L. Gong, L. Huang, F. Luo, R. Krishna, X. F. Yi, A. M. Zheng, L. Zhang, S. Z. Pu, X. F. Feng, M. B. Luo, G. C. Guo, *Angew. Chem. Int. Ed.* **2017**, *56*, 7900–7906; *Angew. Chem.* **2017**, *129*, 8008–8014.
[28] Y. L. Peng, T. Pham, P. F. Li, T. Wang, Y. Chen, K. J. Chen, K. A. Forrest, B. Space, P. Cheng, M. J. Zaworotko, Z. J. Zhang, *Angew. Chem. Int. Ed.* **2018**, *57*, 10971–10975; *Angew. Chem.* **2018**, *130*, 11137–11141.
[29] Y. B. Zhang, L. F. Yang, L. Y. Wang, S. Duttwyler, H. B. Xing, *Angew. Chem. Int. Ed.* **2019**, *58*, 8145–8150; *Angew. Chem.* **2019**, *131*, 8229–8234.
[30] B. Li, X. Cui, D. O'Nolan, H.-M. Wen, M. Jiang, R. Krishna, H. Wu, R.-B. Lin, Y.-S. Chen, D. Yuan, H. Xing, W. Zhou, Q. Ren, G. Qian, M. J. Zaworotko, B. Chen, *Adv. Mater.* **2017**, *29*, 1704210.
[31] Q.-L. Qian, X.-W. Gu, J. Pei, H.-M. Wen, H. Wu, W. Zhou, B. Li, G. Qian, *J. Mater. Chem. A* **2021**, *9*, 9248–9255.
[32] Q. B. Dong, X. Zhang, S. Liu, R. B. Lin, Y. N. Guo, Y. S. Ma, A. Yonezu, R. Krishna, G. P. Liu, J. G. Duan, R. Matsuda, W. Q. Jin, B. L. Chen, *Angew. Chem. Int. Ed.* **2020**, *59*, 22756–22762; *Angew. Chem.* **2020**, *132*, 22944–22950.
[33] Z. Q. Zhang, Q. Ding, J. Y. Cui, X. L. Cui, H. B. Xing, *Small* **2020**, *16*, 2005360.
[34] Z. Zhang, S. B. Peh, R. Krishna, C. Kang, K. Chai, Y. Wang, D. Shi, D. Zhao, *Angew. Chem. Int. Ed.* **2021**, *60*, 17198–17204.
[35] W. Yang, A. J. Davies, X. Lin, M. Suyetin, R. Matsuda, A. J. Blake, C. Wilson, W. Lewis, J. E. Parker, C. C. Tang, M. W. George, P. Hubberstey, S. Kitagawa, H. Sakamoto, E. Bichoutskaia, N. R. Champness, S. Yang, M. Schroder, *Chem. Sci.* **2012**, *3*, 2993–2999.
[36] L. Li, J. Wang, Z. Zhang, Q. Yang, Y. Yang, B. Su, Z. Bao, Q. Ren, *ACS Appl. Mater. Interfaces* **2019**, *11*, 2543–2550.

Manuscript received: July 22, 2021
Revised manuscript received: August 25, 2021
Accepted manuscript online: August 29, 2021